The Photon Reactor:
Producing Power By Burning Nuclear Waste

Paul M. Brown, Ph.D.
Nuclear Solutions, LLC

SUMMARY

A linear accelerator, preferably of the monochromatic type, accelerates electrons which are directed onto a high Z target such as tungsten to generate gamma rays about 9 MeV, which are directed onto the fuel material such as U-238 which results in the (γ,*f*) reaction, thus releasing about 200 MeV. A reactor built according to this principle requiring an accelerator driven by 1 MW will develop about 20 MW of power. The reaction is not self-sustaining and stops when the beam is turned off. This accelerator driven reactor may be used to "burn-up" spent fuel from fission reactors, if simply operated at 10 MeV. The photo-fission results in typical spent fuel waste products such as Cs^{137} and Sr^{90} which undergo photodisintegration by the (γ,n) reaction resulting in short lived or stable products. Chemical separations of the spent fuel isotopes is not necessary. Of course, more than one accelerator may be used to drive the reactor to higher power levels, and speed-up the burn-up process. The fact that the reaction is not self-sustaining is a safety feature allowing immediate shut-down in the event of a problem.

INTRODUCTION

The nuclear fission of heavy elements following the absorption of electromagnetic radiation (photofission) was first predicted by Bohr and Wheeler (ref 1) in their famous 1939 paper. Haxby, Shoupp, Stephens, and Wells (1941) were the first to produce fission with gamma rays.

A survey of the literature indicates that photonuclear reaction studies in actinide nuclei have been the pursuit of several laboratories, during the last 40 years, using several types of gamma sources. The main objective of these studies has been to obtain nuclear information at excitation energies in the region of the giant dipole resonance and in the region of low energy, near the photofission and photoneutron thresholds.

Bowman (ref 4) using a quasi-monochromatic photon beam obtained from the anihilation in flight of monochromatic positrons, was the first to observe the characteristic splitting, of the giant dipole resonance, of a fissile nucleus into two components, a phenomenon observed for other permanently deformed nuclei as well (ref 6). However, they found that the photon-induced Γ_n/Γ_f ratio was strongly energy dependent, a result in complete disagreement with data obtained from neutron-induced fission, bremsstrahlung-induced fission and charged-particle-induced fission (ref 5).

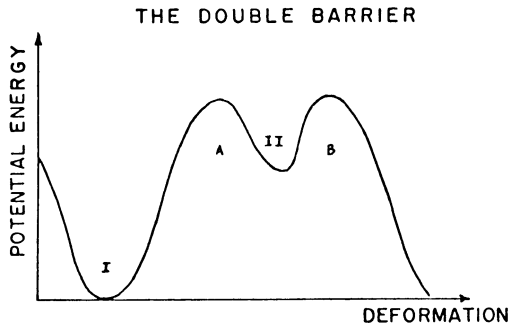

Figure 1. The characteristic double-humped curve typical of strongly deformed nuclei.

It is well known that at neutron number N = 90 a sharp change in the nuclear surface properties occurs. The resulting transition from equilibrium spherical to prolate nuclear shape leads to a change in the nuclear optical anisotropy and, consequently, in the shape of the giant resonance in the photoabsorption cross section as shown in Figure 1. Since many nuclear properties depend similarly on the proton and neutron numbers, it is reasonable to expect that analogous transition effects should be observed for Z = 90 nuclei as well, which will lead to the evolution of their photoabsorption cross section shape (ref 7). This giant-resonance absorption is ascribed to the excitation of dipole vibrations of all the protons against all the neutrons in the nucleus, the protons and neutrons separately behaving as compressible fluids. This model makes some fairly simple predictions about the magnitude and A-dependence of the resonance that are quite well borne out by the experimental data: the integrated cross sections under the resonance peaks are given to good approximation by 0.06NZ/A MeV b, and the peak energies can be approximately represented by $aA^{-1/3}$.

The energy of the dipole resonance is so low that mostly rather simple processes-such as (γ, *n*) and photofission reactions-take place in the giant-resonance region. The competition between these processes is governed by the usual statistical considerations of compound-nucleus de-excitation, so that neutron emission usually dominates.

The characteristics of the giant dipole resonance for the actinide nuclei are of particular interest. For such high-Z, high-Coulomb barrier nuclei, the total photon-absorption cross section is equal to the sum of the photoneutron and photofission cross sections. The total photoneutron cross section is the sum of the following reaction cross sections,

$$\sigma(\gamma, n_{tot}) = \sigma(\gamma,n) + 2\sigma(\gamma,2n) + \nu\sigma(\gamma,f) \qquad \text{(Eq. 1)}$$

where ν is the neutron multiplicity of a fission event. The total neutron production cross section is then,

$$\sigma_{\gamma,N} = \sigma_{\gamma,n} + \nu\sigma_{\gamma,f} \qquad \text{(Eq. 2)}$$

The competition between neutron emission and fission may be expressed,

$$\Gamma n/\Gamma f\,(E) = \sigma(\gamma,n)/\sigma(\gamma,f)(E) \qquad \text{(Eq. 3).}$$

The value for Γn/Γf decreases exponentially with the fissility of the nuclei (ref 8). The theoretical expression for Γn/Γf which explains this behavior for the neutron emission and fission competition is derived from the Constant Nuclear Temperature for the level density, and is expressed.

$$\Gamma n/\Gamma f = 2\ TA^{2/3}/10 \exp\{(Ef' - Bn')/T\} \qquad \text{(Eq. 4)}$$

where (Ef' - Bn') are the effective thresholds for the respective photonuclear processes and T is the nuclear temperature.

The fact that more than one neutron is emitted per fission in the fission of such isotopes as Th^{232}, U^{233}, U^{235}, U^{238}, and Pu^{239} leads to the possibility of a chain reaction in a mass of fissionable material. Whether the chain reaction remains steady, builds up, or dies down depends upon the competition between the production of neutrons through fission and the loss of neutrons through a variety of processes such as non-fission capture of neutrons, primarily (n,γ) reactions in the system, and the leakage of neutrons through the surface of the system.

Energy is released at the rate of 200 MeV per fission of one atom or about 23 X 10^6 kw-hr per fission of one kilogram of U^{235}. The fission fragments carry off 82% of the energy in the form of kinetic energy. Prompt neutrons carry off another 2.5%, prompt gammas carry off 3.5%, beta decay accounts for 4%, delayed gammas account for 3%, and neutrinos carry off the remaining 5%. The neutrinos and their energy are lost, since the probability of interaction with neutrinos is so small. Some fission also occurs as a fast neutron strikes a U^{238} atom. Also, as the fuel is burned, plutonium is produced, and by the end of a fuel cycle (18 months of operation), 35% of the energy is actually coming from the fission of Pu^{239} atoms. About 80% of the neutron absorption in U^{235} results in fission; the other 20% are (n,γ) reactions.

Once a fission chain reaction is started, the *effective multiplication factor* k_e will determine whether the chain reaction will continue at a steady rate, increase, or decrease. The effective multiplication factor is defined as *the ratio of the rate of production of neutrons,* P, *to the combined rate of absorption* A *and the rate of leakage* L *of neutrons,* or k_e = P/A+L. The term *absorption* includes all types of absorption, such as those which produce fission and those which produce (n,γ) processes in the material of the reactor. The fission chain reaction will be critical or steady when k_e=1, it will be building up or *supercritical* when k_e>1, and it will be dying down or *subcritical* when k_e <1.

If F is the rate at which fission processes occur, and if ν is the average number of neutrons emitted per fission, then P=νF. Then we may write k_e = P/A+L as k_e=νF/A+L from which we get

$$k_e = \nu(F/A)\ [1/1+(L/A)] \qquad \text{(Eq. 5).}$$

The ratio F/A depends upon the amount of fissionable and nonfissionable material and on their cross sections for fission and neutron capture. The ratio L/A depends upon the ability of the reactor to contain and absorb neutrons before they can escape through the surface. As the size of a reactor decreases, the rate of neutron leakage through the surface increases, and the rate of neutron absorption decreases, so that L/A increases and approaches infinity, and hence in the limit k_e approaches zero. As the size of the reactor

increases, L/A decreases toward zero, and k_e increases toward the limiting value νF/A. Hence if the composition of the reactor is such that νF/A>1, then there is some size of this reactor for which k_e=1; for this size, the reactor is critical. This size is called the *critical size* and the mass of fissionable material at this size is called the *critical mass*. The region containing the fissionable material is called the *reactor core*. The core may be surrounded by nonfissionable material capable of reflecting neutrons back into the core; in such a case both the critical size and the critical mass are reduced. On the other hand, if there is an insufficient amount of fissionable material or an excess of absorbing material in the reactor core so that νF/A<1, then there is no size for which a steady chain reaction can occur, irrespective of whether or not a reflector is used. Pure natural uranium, no matter how large the amount, cannot support a chain reaction, that is νF/A<1.

Table I-Thermal Neutron Cross Sections For Uranium

Process	Cross Section (Barns)		
	U^{235}	U^{238}	$U^{natural}$
Fission	549	0	3.92
n-Capture	101	2.80	3.5
Scattering	8.2	8.2	8.2

Titterton (1950) found that the average kinetic energy released in the photofission of Th^{232} is about 0.8 of that released in the slow-neutron fission of U^{235} or about 160 MeV.

Table II-Fission Threshold Energy of Select Isotopes

NUCLIDE	PHOTOFISSION THRESHOLD (MeV)	NEUTRON-FISSION THRESHOLD (MeV)
Am^{241}	6.0	--
Am^{242}	--	6.4
Th^{232}	5.8	1.3
Np^{237}	5.6	0.4
Np^{238}	--	6.0
U^{233}	5.7	0.025
U^{234}	6.0	0.4
U^{235}	5.3	0.025
U^{236}	--	0.8
U^{237}	--	6.3
U^{238}	5.8	1.2
Pu^{239}	5.8	0.025

THE NUCLEAR WASTE PROBLEM

A typical 1000 MWe PWR reactor operating at 75% capacity generates about 21 tons of spent fuel at a burn-up of 43 GWd/t. The 21 tons of spent fuel (contained inside 42 PWR fuel elements with a total volume of about 11 m^3) will have produced an electric energy of about 6.6 TWh (6.6 billion kWh). This same energy output corresponds to the burning of 2 million tons of coal in a conventional power plant giving rise to 120,000 tons of ashes, 5.4 million tons of CO_2 and 50,000 tons of SO_2.

Spent fuel consists of uranium which accounts for about 96% of the spent fuel removed from commercial nuclear reactors. In the case of light water reactors (the type most commonly used) the spent fuel contains 0.90% U^{235} whereas natural uranium contains only 0.70% of this isotope. Plutonium constitutes about 1% of the weight of spent fuel, it is fissile which means that it can be used as fuel in nuclear reactors. The minor actinides constitute about 0.1% of the weight of spent fuel. They consists of about 50% Np, 47% Am and 3% Cm which are very radiotoxic. The fission products (iodine, technetium, neodymium, zirconium, molybdenum, cerium, cesium, ruthenium, palladium, etc.) constitute about 2.9% of the weight of spent fuel.

The two fission products of principal concern because of their substantial thermal impact on the repository as opposed to posing a health risk are Sr^{90} and Cs^{137}. These two radionuclides are dominant contributors to the heat released by spent fuel at least for the first several decades. Cs^{137} is also a major source of penetrating radiation emitted by spent fuel. The two fission products of principal concern because of their potential contribution to health risk are Tc^{99} and I^{129}. They are of principal concern because they are long-lived, produced in significant amounts in the fission process, generally soluble under geologic conditions, and migrate relatively quickly under common ground water conditions.

The long-term toxicity of spent fuel is dominated by the actinides such as Np^{237}, $U^{234,236}$, and $Pu^{239,240,242}$. The transmutation of long-lived nuclides in high level waste to stable or short-lived nuclides by stimulating nuclear reactions is a desirable alternative approach for the reduction of high level waste.

There are about 300 different radioactive species generated by the operation of a nuclear reactor, primarily as a result of neutron capture and neutron-induced fission. The adverse impact of the various radionuclides varies because of the differences in the chemical behavior in the body of, and the radiation emitted by, the radionuclides. The risk focus of the radionuclides is related to waste disposal in a geologic repository. The most common release and exposure mechanisms from a repository involve ground water contacting the waste form followed by slow dissolution, transport of radionuclides to the accessible environment, distribution in the biosphere, and eventual uptake from food and water. Although hundreds of isotopes are present in spent fuel or wastes derived from them, only a few of them are important for disposal. These four isotopes Cs^{137}, Sr^{90}, I^{129} and Tc^{99} are the primary focus of concern for light-water reactor spent fuel, i.e., nuclear waste due to their excess heat, groundwater solubility, or health risk.

The management of spent fuel should ensure that the biosphere is protected under economically acceptable conditions without entailing unfavorable short-term consequences and the public must be convinced of the effectiveness of the methods. Since the spent fuel contains very long-lived radionuclides, some protection is required for at least 100,000 years. Two means are possible:

1. We can wait for the natural decay of the radioactive elements by isolating them physically from the biosphere by installing successive barriers at a suitable depth in the ground. This strategy is called deep geological disposal;

2. We can make use of nuclear reactions that will transmute the very long-lived wastes into less radioactive or shorter-lived products. This strategy is called transmutation (ref 11).

The problem with storing nuclear waste below ground is that there is no material that will outlast its radioactive contents and radioactive wastes continuously produce heat, hydrogen and helium outgassing, as well as other labile products.

The nuclear industry with the federal government have spent more than $6 billion in development of the Yucca Mountain, Nevada, site where they plan to store 77,000 metric tons of high-level radioactive waste. A June 29, 1992, earthquake of 5.9 magnitude on the Richter scale, caused $1 million in damage to a Department of Energy building six miles from the proposed Yucca Mountain site. DOE scientists were rattled to discover that the epicenter of the quake was 12 miles from the proposed dump site. Senator Richard Bryan (Democrat Nevada) said, "Mother Nature delivered a wake-up call to America's policy makers. Placing…high-level radioactive nuclear waste in an active earthquake zone defies common sense."

In 1991, mining experts reported that a deep underground salt chamber (Waste Isolation Pilot Plant or WIPP) in the New Mexico desert designated for the first US tests of permanent radioactive waste disposal would probably collapse years before the tests could be completed. Currently, the WIPP facility is to start accepting waste January 1999.

There are some 114 nuclear reactors in the United States and about 400 commercial nuclear power plants in operation around the world including about 120 GWe nuclear electric capacity in Western Europe and 45 GWe operational in the ex-USSR and East European countries. In the US alone, we have accumulated 34,000 tons of nuclear waste. The current US production rate of high-level waste (primarily spent fuel) is 3,000 tons per year. The average commercial power plant puts 60 used fuel assemblies into "temporary" storage each year and is expected to do so until the year 2000 when the waste is to be transferred to DOE. This does not include low-level wastes such as gloves, filters, tools, clothing, etc., that come from nuclear power plants, research centers, and hospitals that use radioactive materials. There are about 100,000 US facilities that use radioactive materials. They produce 1.6 million cubic feet of low-level waste each year.

Current projected costs of the US Environmental Management program are about $7.5 billion per year. Paper studies currently account for about 20% of the Environmental Restoration budget. According to the Baseline Environmental Management Report, the total clean-up cost of the nuclear weapons program is $230 billion over a 75 year period, including the $50 billion projected Hanford clean-up.

THE SOLUTION: SUB-CRITICAL ACCELERATOR DRIVEN REACTOR

The photon reactor is a method and means for producing nuclear energy from heavy elements but not fissile elements. The reaction is not driven by the well known self-sustained, chain-reaction, of U^{235}, rather by an accelerator. The fuel for this type of accelerator driven reactor may be the spent fuel from fission reactors. The mechanism by which nuclear energy is released from non-fissile material is known as photo-fission, wherein a photon or gamma is introduced greater than the photo-fission threshold energy resulting in fission of the target nucleus. For instance, with U^{238}, the threshold of photo-fission is about 6 MeV and results in fission of the U^{238} nucleus releasing about 200 MeV. Patents are currently pending.

A linear accelerator, preferably of the monochromatic type, accelerates electrons which are directed onto a high Z target such as tungsten to generate gamma rays of an

energy about 10 MeV, which are directed onto the fuel material such as U^{238} which results in the (γ,*f*) reaction, thus releasing about 200 MeV. A reactor built according to this principle requiring an accelerator driven by 1 MW will develop about 20 MW of power. The reaction is not self-sustaining and stops when the beam is turned off. This accelerator driven reactor may be used to "burn-up" spent fuel from fission reactors, if simply operated at 10 MeV. The photo-fission results in typical spent fuel waste products such as Cs^{137} and Sr^{90} which undergo photodisintegration by the (γ,n) reaction resulting in short lived or stable products. Chemical separations of the spent fuel isotopes is not necessary. Of course, more than one accelerator may be used to drive the reactor to higher power levels, and speed-up the burn-up process. Ideally, four spaced accelerators would require about 4.8 MW of power to run resulting in about 100 MW from the reactor.

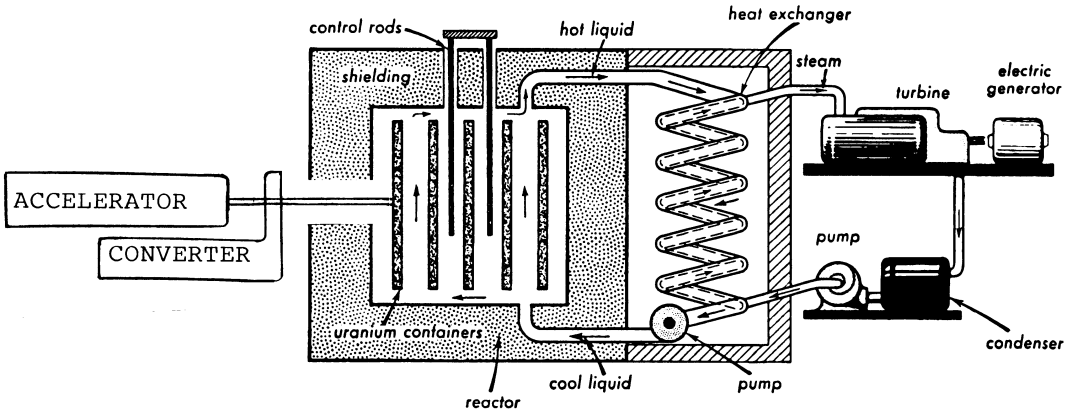

Figure 2. The accelerator driven reactor schematic.

REACTIONS IN THE ACCELERATOR DRIVEN REACTOR

It is important to note that although the reactor is sub-critical and driven by gamma rays, the neutrons produced still induce both fast and slow neutron fission just as in any conventional reactor. These neutron reactions result in additional energy output thereby increasing the input/output ratio from 1/20 a value determined by the design.

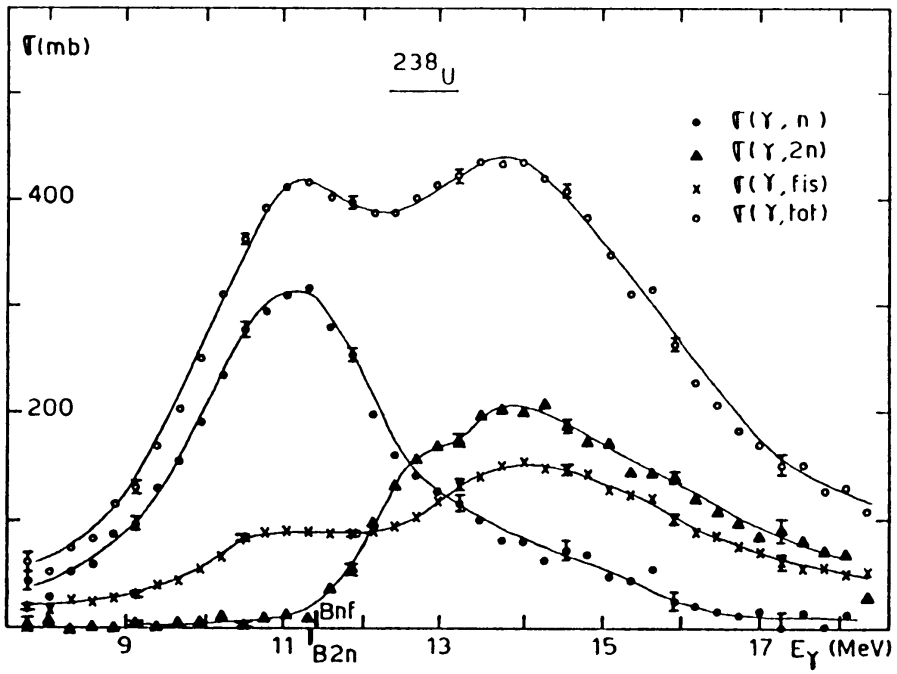

Figure 3. Partial and total photonuclear cross sections (γ,n), (γ,2n), (γ,f), and (γ,tot) for U^{238}.

Figure 3 shows the photonuclear cross sectional data obtained by Veyssiere (ref 5) for U^{238}. Notice that the total photonuclear cross sections all have about the same peak cross section value. The maximum cross sections are all about 0.5 b and all are about 6 MeV wide, this appears to hold true for all the actinides. The photo-absorption cross section falls sharply above the (γ,2N) and (γ,nf) peaks, as is the case for essentially all medium and heavy nuclei as provided by the examples in figure 4.

The thermal fissionable nuclides include Np^{238}, Pa^{232}, Pu^{239}, Pu^{241}, Th^{227}, U^{231}, U^{233}, U^{235}. All those nuclides fissionable by thermal neutrons are, of course, also fissionable by fast neutrons. In addition, there are several nuclides such as U^{238}, Th^{232}, Pa^{231}, and Np^{237} which are fissionable by neutrons having energies of about 1 MeV.

Looking at figures 3 through 5 we see that at 10 MeV the (γ,n) reaction is about three times the (γ, *f*) reaction. Table IV lists several (γ,n) reactions that result in the neutralization or burn-up of the radioisotope resulting in stable, non-radioactive products.

The reactions that occur within the accelerator driven reactor are too numerous to list but the most important reactions are shown in Table IV (ref 14).

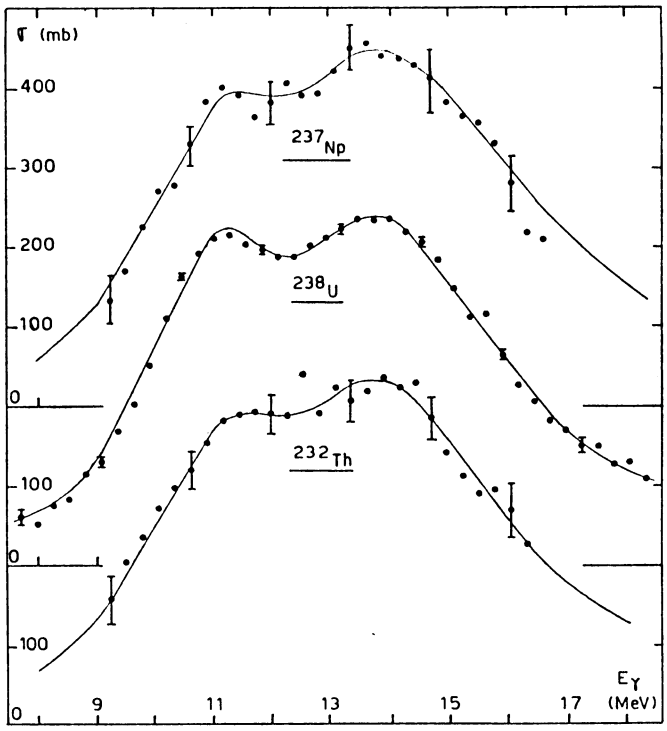

Figure 4. Total photonuclear cross sections for Th^{232}, U^{238} and Np^{237}.

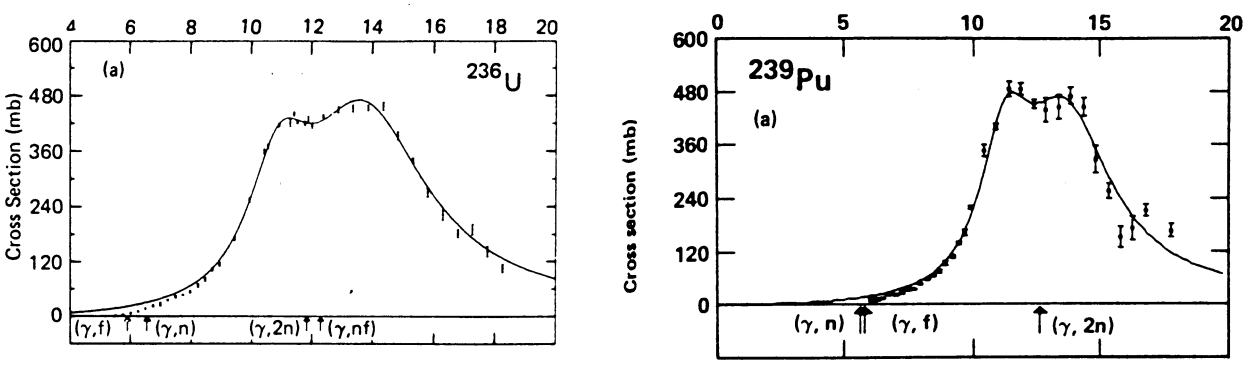

Figure 5. Total photonuclear cross section for U^{236} and Pu^{239}.

Table III-Fissionabilities

Nucleus	Z^2/A	$\sigma_{int}(\gamma,F)/\ \sigma_{int}(\gamma,tot)$	Γ_n/Γ_f
Th^{232}	34.91	0.11	15
U^{238}	35.56	0.30	3.9
U^{236}	35.86	0.46	2.1
U^{235}	36.02	0.62	1.4
U^{234}	36.17	0.68	0.99
U^{233}	36.33	0.81	0.49
Np^{237}	36.49	0.60	0.68
Pu^{239}	36.97	0.74	0.62

Table IV-Relevant Reactions in Photon Driven Reactor

PHOTOFISSION REACTIONS:

(γ, *f*): U^{238}, Th^{232}, Pa^{231}, Np^{237}, Np^{238}, Pa^{232}, Pu^{239}, Pu^{241}, Th^{227}, U^{231}, U^{233}, U^{235}.

FISSION REACTIONS: (just one of many)

$$_{92}U^{235} + {}_{0}n^{1} \rightarrow {}_{38}Sr^{94} + {}_{54}Xe^{140} + 2\ {}_{0}n^{1}$$
$$_{38}Sr^{94} \rightarrow {}_{39}Y^{94} + \beta^{-} \rightarrow {}_{40}Zr^{94} + \beta^{-} \text{ (stable)}$$
$$_{54}Xe^{140} \rightarrow {}_{55}Cs^{140} + \beta^{-} \rightarrow {}_{56}Ba^{140} + \beta^{-} \rightarrow {}_{57}La^{140} + \beta^{-} \rightarrow {}_{58}Ce^{140} + \beta^{-} \text{ (stable)}$$

(γ,n) ENRICHMENT:

$$_{92}U^{236} + \gamma \rightarrow {}_{92}U^{235} + {}_{0}n^{1}$$
$$_{92}U^{238} + \gamma \rightarrow {}_{92}U^{236} + 2\ {}_{0}n^{1} + \gamma \rightarrow {}_{92}U^{235} + {}_{0}n^{1}$$
$$_{95}Am^{241} + \gamma \rightarrow {}_{95}Am^{240} + {}_{0}n^{1} + {}_{-1}e^{0} \rightarrow {}_{94}Pu^{240}$$
$$_{93}Np^{237} + \gamma \rightarrow {}_{93}Np^{235} + 2\ {}_{0}n^{1} + {}_{-1}e^{0} \rightarrow {}_{92}U^{235}$$
$$_{92}U^{238} + \gamma \rightarrow {}_{92}U^{237} + {}_{0}n^{1} + \gamma \rightarrow {}_{92}U^{236} + {}_{0}n^{1} + \gamma \rightarrow {}_{92}U^{235} + {}_{0}n^{1}$$
$$_{94}Pu^{238} + \gamma \rightarrow {}_{94}Pu^{236} + 2\ {}_{0}n^{1} + \gamma \rightarrow {}_{94}Pu^{235} + {}_{0}n^{1} + {}_{-1}e^{0} \rightarrow {}_{93}Np^{235} + {}_{-1}e^{0} \rightarrow {}_{92}U^{235}$$
$$_{92}U^{238} + \gamma \rightarrow {}_{92}U^{237} + {}_{0}n^{1} \rightarrow {}_{93}Np^{237} + \beta^{-} + \gamma \rightarrow {}_{93}Np^{235} + 2\ {}_{0}n^{1} + {}_{-1}e^{0} \rightarrow {}_{92}U^{235}$$
$$_{94}Pu^{239} + \gamma \rightarrow {}_{94}Pu^{237} + 2\ {}_{0}n^{1} + \gamma \rightarrow {}_{94}Pu^{235} + 2\ {}_{0}n^{1} + {}_{-1}e^{0} \rightarrow {}_{93}Np^{235} + {}_{-1}e^{0} \rightarrow {}_{92}U^{235}$$
$$_{94}Pu^{239} + \gamma \rightarrow {}_{92}U^{235} + \alpha$$

NEUTRON ENRICHMENT:

$$_{92}U^{234} + {}_{0}n^{1} \rightarrow {}_{92}U^{235} + \gamma$$
$$_{92}U^{238} + {}_{0}n^{1} \rightarrow {}_{92}U^{239} + \gamma \rightarrow {}_{93}Np^{239} + \beta^{-} \rightarrow {}_{94}Pu^{239} + \beta^{-}$$
$$_{90}Th^{232} + {}_{0}n^{1} \rightarrow {}_{90}Th^{233} + \gamma \rightarrow {}_{91}Pa^{233} + \beta^{-} \rightarrow {}_{92}U^{233} + \beta^{-}$$

(γ,n) NEUTRALIZATION:

$$_{1}H^{3} + \gamma \rightarrow {}_{1}H^{2} + {}_{0}n^{1} \text{ (stable)}$$
$$_{6}C^{14} + \gamma \rightarrow {}_{6}C^{13} + {}_{0}n^{1} \text{ (stable)}$$
$$_{39}Y^{90} + \gamma \rightarrow {}_{39}Y^{89} + {}_{0}n^{1} \text{ (stable)}$$
$$_{28}Ni^{63} + \gamma \rightarrow {}_{28}Ni^{62} + {}_{0}n^{1} \text{ (stable)}$$
$$_{36}Kr^{85} + \gamma \rightarrow {}_{36}Kr^{84} + {}_{0}n^{1} \text{ (stable)}$$
$$_{27}Co^{60} + \gamma \rightarrow {}_{27}Co^{59} + {}_{0}n^{1} \text{ (stable)}$$
$$_{81}Tl^{204} + \gamma \rightarrow {}_{81}Tl^{203} + {}_{0}n^{1} \text{ (stable)}$$
$$_{38}Sr^{90} + \gamma \rightarrow {}_{38}Sr^{88} + 2\ {}_{0}n^{1} \text{ (stable)}$$
$$_{83}Bi^{210} + \gamma \rightarrow {}_{83}Bi^{209} + {}_{0}n^{1} \text{ (stable)}$$
$$_{56}Ba^{133} + \gamma \rightarrow {}_{56}Ba^{132} + {}_{0}n^{1} \text{ (stable)}$$
$$_{82}Pb^{210} + \gamma \rightarrow {}_{82}Pb^{208} + 2\ {}_{0}n^{1} \text{ (stable)}$$
$$_{38}Sr^{90} + \gamma \rightarrow {}_{38}Sr^{89} + {}_{0}n^{1} \rightarrow {}_{39}Y^{89} + \beta^{-} \text{ (stable)}$$
$$_{53}I^{129} + \gamma \rightarrow {}_{53}I^{128} + {}_{0}n^{1} \rightarrow {}_{54}Xe^{128} + \beta^{-} \text{ (stable)}$$
$$_{55}Cs^{137} + \gamma \rightarrow {}_{55}Cs^{136} + {}_{0}n^{1} \rightarrow {}_{56}Ba^{136} + \beta^{-} \text{ (stable)}$$
$$_{26}Fe^{60} + \gamma \rightarrow {}_{26}Fe^{59} + {}_{0}n^{1} \rightarrow {}_{27}Co^{59} + \beta^{-} \text{ (stable)}$$
$$_{82}Pb^{210} + \gamma \rightarrow {}_{82}Pb^{209} + {}_{0}n^{1} \rightarrow {}_{83}Bi^{209} + \beta^{-} \text{ (stable)}$$

Table IV-Relevant Reactions in Photon Driven Reactor, cont.

In a (γ, n) reaction neither the γ-ray nor the neutron has a Coulomb barrier to surmount, so reaction sets in sharply as soon as the threshold energy is reached (ref 13).

For many fission products the neutron capture cross sections in a thermal spectrum can give substantial transmutation rates. The transmutation of Tc^{99} is characteristically much more effective in a thermal neutron spectrum generally due to higher neutron capture cross section at lower energies.

The systematics of the giant dipole resonance, which characterizes the absorption of electromagnetic radiation by nuclei in the energy range from about 5 to 30 MeV, have been of interest since the discovery of the giant resonance itself. Over the years, the photoneutron cross sections for many nuclei have been measured with monoenergetic photons in numerous laboratories. All these data are presented in the Atomic Data Nuclear Data Tables. For most cases studied, the agreement is remarkably good.

THE ACCELERATOR

The high-energy x-ray machine requires a high-power, low-energy (10 MeV) electron linac to produce the gamma rays to drive the reactions in the reactor. Current technology suggests the use of a traveling wave resonant ring (TWRR) accelerator energized by two 1.2 MW continuous wave (CW) L-band klystrons (1249 MHz RF) to produce an electron beam with an energy of 10 MeV and a current of 100 mA. The average beam power is 200 kW-1 MW for the duty factor 20-100%. At full beam loading the accelerator is 65% efficient and is operable at room temperature.

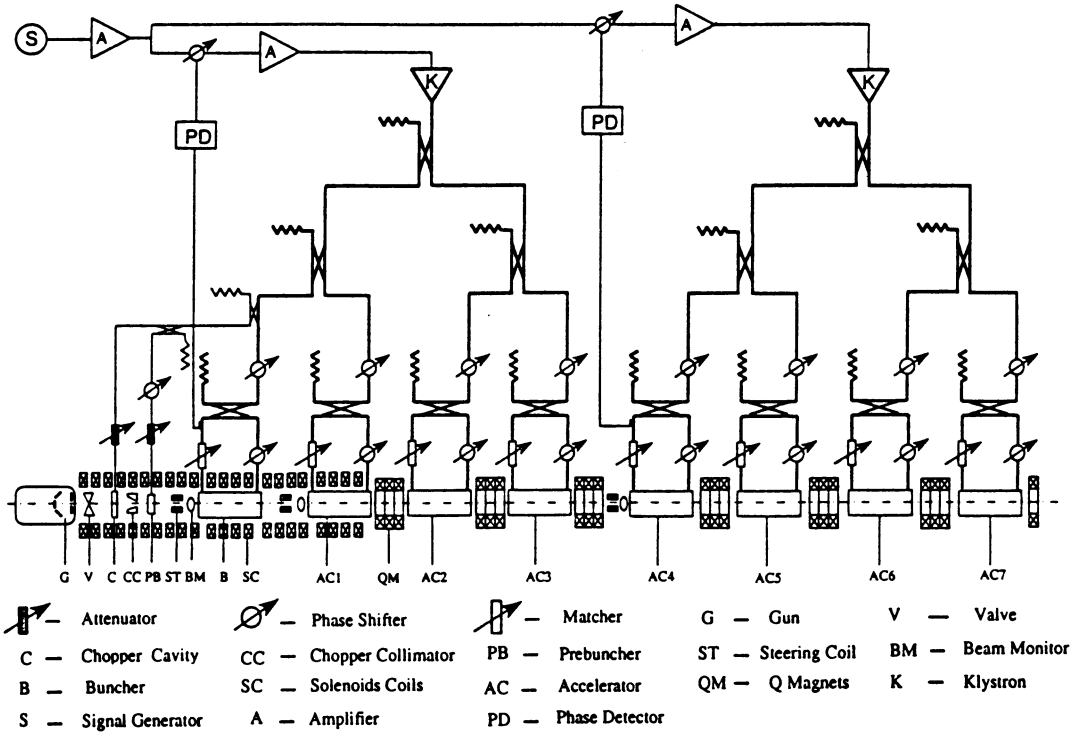

Figure 6. Schematic layout of CW electron linac (ref 19).

The TWRR was selected to enhance the threshold current of beam break-up and to get high accelerator efficiency that results from the low value of attenuation constant and

high field multiplication factor which are permitted only with TWRR. The advantages of using TWRR rather than a standing wave accelerator guide are; simplicity of cavity structure, larger aperture size, ease of fabrication, and easy mechanical separation from the recirculating wave guide. All these things make it easy to handle under a high radiation field.

The klystrons are driven by 90 KVDC power supply to produce 1.2 MW RF with the efficiency of more than 65%. The 1.2 MW RF power is fed into four TWRR through two 3 dB directional couplers.

The injector consists of a 200 KVDC electron gun, two magnetic lenses, a RF chopper, a chopper slit, a prebuncher and a buncher. A peak current of 400 mA with beam energy of 200 KeV is required for the electron gun from the chopper and the buncher system design.

The accelerator section consists of seven accelerator guides. Each unit of accelerator section forms a TWRR. Each of the accelerator guides of which the length is 1.2 m, contains 13 $2\pi/3$ mode cavities and two coupling cavities. All accelerator guides are constant gradient structure types under the condition of 100 mA beam loading. A straight waveguide was used instead of a phase shifter.

The first klystron energizes a buncher and three accelerator guides while the second klystron energizes the remaining four accelerator guides. The RF power fed into the buncher and each accelerator guide are 220 to 250 KW, respectively.

Table V summarizes the characteristics of the 1 MW beam linac used at PNC.

Table V-Accelerator Specifications (ref 19)

General	
Operation Mode	Continuous Wave
Energy	10 MeV
Beam Current	100 mAmp
Total Length	18 meters
Normal Emittance	50% mm mrad
Energy Spread	1%
Accelerator Section	
Type	Traveling Wave Constant-Gradient
Mode	$2\pi/3$
Frequency	1249.135 MHz
Gain (max)	1.4 MV/m to 2.0 MV/m
Number of Accelerator Guides	7
Resonant Ring	
Transmission (no load)	0.946
Transmission (load)	0.850
Multiplication (no load)	3.0
Multiplication (load)	2.0
Klystron	
Number of klystrons	2
Power	1.2 MW
Beam Voltage	90 KV

Micro-Perveance	0.8
Gain	50 dB
Efficiency	65%
Modulation	Modulating Anode

BEAM FLUX REQUIREMENTS

Calculations show that efficient (γ,n) incineration of Cs^{137} and Sr^{90} requires a gamma flux of but only 10^{18} γ/cm^{2}sec to accelerate the time of decay by 180 times (ref 21).

The number of nuclei (γ,n) reacting during the irradiation can be determined by the following differential equation:

$$dN_i/dt = -(\lambda_i + \sigma_i \phi) N_i + \sum_{j \neq i}^{N_a} (\lambda_{ji} + \sigma_{ji} \phi) N_j, \qquad \text{(Eq. 6)}$$

$$i = 1,2,\ldots, N_a$$

where

N_i = number of the ith nucleus,
λ_i = decay constant of the ith nucleus,
σ_i = total photonuclear cross section of the ith nucleus
λ_{ji} = decay constant from the jth nucleus transmuting to the ith one,
ϕ = γ-ray flux,
N_a = number of nuclei considered in the model.

Using the matrix representation, eq.(6) is written as follows:

$$d\mathbf{N}/dt = \mathbf{A} \bullet \mathbf{N}, \qquad \text{(Eq. 7)}$$

where

$$A_{ji} = \begin{cases} -(\lambda_i + \sigma_i \phi) & (i = j), \\ \lambda_{ji} + \sigma_{ji} \phi & (i \neq j). \end{cases}$$

The matrix of the nuclei **N** at the time t=Δt can be obtained by the Taylor's expansion:

$$\mathbf{N}(t + \Delta t) = \mathbf{N}(t) + \sum_{r=1} (\Delta t)^r /r!\ d\mathbf{N}^{(n)}(t)/dt, \qquad \text{(Eq 8)}$$

where

$d\mathbf{N}^{(n)}(t)/dt$ is the rth derivative of $\mathbf{N}(t)$.

Combining equations (7) and (8), we can obtain $\mathbf{N}(t+\Delta t)$ as follows:

$$\mathbf{N}(t + \Delta t) = \mathbf{N}(t) + \sum_{r=1} (\Delta t)^r/r!\ \mathbf{A}^r\mathbf{N}(t). \qquad \text{(Eq. 9)}$$

The matrix **A** contains two kinds of data: the decay constants and the photonuclear cross sections.

Figure 8 shows the products produced by photofission of Uranium-238 by 10 MeV x-rays (ref 15). The U^{238} itself may be used as both the gamma converter and the target, that is, eliminate a separate electron to gamma converter and use the target material itself as the x-ray source. The advantage here is the recovery of the heat normally dissipated in the converter which is on the order of 70% of the beam energy (ref. 22).

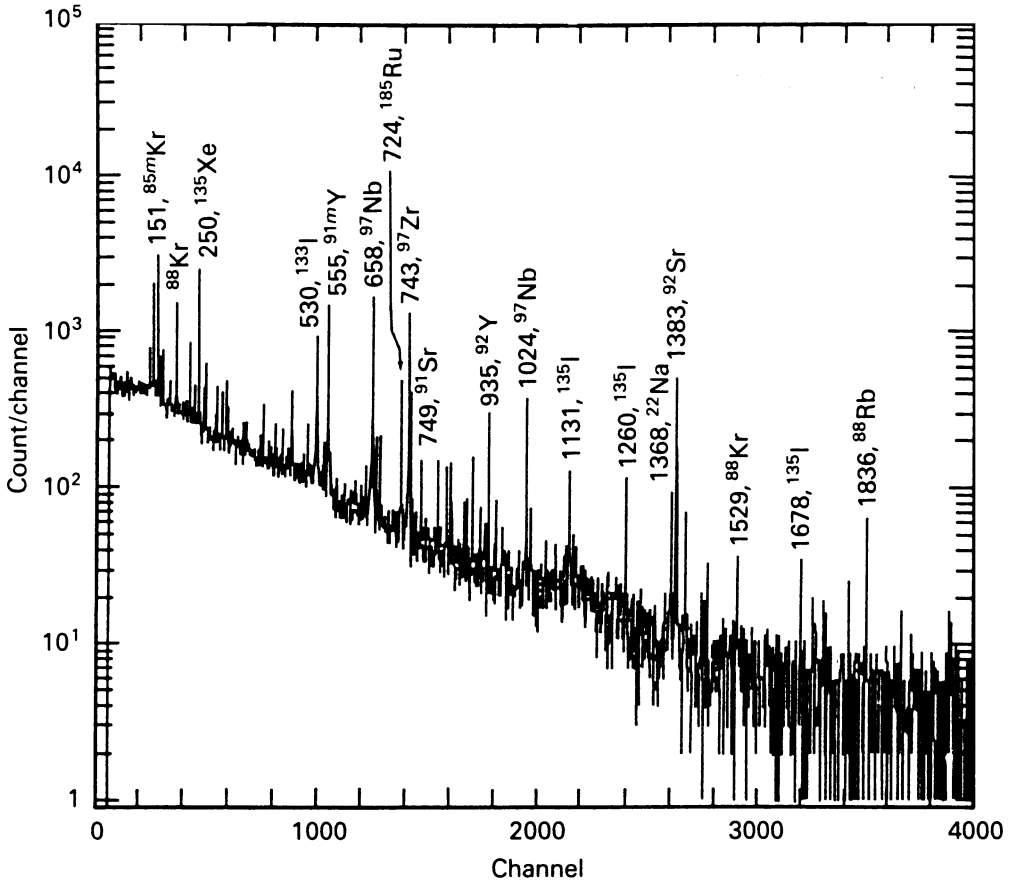

Figure 8. Products produced by photofission of U^{238} target with 10 MeV photons.

CONCLUSION

The (γ, *f*) and (γ,n) incineration of spent nuclear fuel provides an efficient and reasonable method for disposal of radioactive waste while providing a relatively cheap and safe source of power at the same time. No new technology needs to be developed since we currently have all the required technology available to us. A small proof of principle accelerator driven reactor could be build using known engineering with reasonable assurance and confidence that it will work as designed. Such a reactor may be fueled by current nuclear waste stockpiles, spent nuclear fuel, natural U^{238} or natural Th^{232}. Matsumoto ran the calculations to show it is theoretically feasible; Kase ran the feasibility experiment that provided proof of feasibility on the laboratory scale; Safety is high, fuel is cheap and abundant, now all that remains is to apply the technology and build an experimental accelerator driven reactor.

REFERENCES

1. 1. N. Bohr and J. Wheeler, Phys. Rev. 56, 426 (1939).
2. E. Hyde, *The Nuclear Properties of the Heavy Elements*, Vol. 3, (Prentice Hall, Englewood Cliffs, NJ, 1964)
3. J. Caldwell, et.al., *Giant Resonance for the Actinide Nuclei: Photoneutron and Photofission Cross Sections for U^{235}, U^{236}, U^{238} and Th^{232}*, Phys. Rev. C21, No. 4, p. 1215-1231, April 1980.
4. C. Bowman, et.al., Phys. Rev. 133, B676 (1964).
5. A. Veyssiere, et.al., *A Study of the Photofission and Photoneutron Processes in the Giant Dipole Resonance of Th^{232}, U^{238} and Np^{237},* J. Nuclear Physics A199, 45, 7301 (1973).
6. R. Bergere, et.al., Nucl. Phys. A121, 463 (1968).
7. G. Gurevich, et.al., *Giant Resonance in the Total Photoabsorption Cross Section of Z = 90 Nuclei*, Nucl. Phys. A273, p. 326-340 (1976).
8. M. Cesar, et.al., *Photoneutron Cross Sections of Pu-239 Using Neutron Capture Gamma Rays, Near Threshold,* Physica Scripta 47 (1992).
9. B. Berman, *Photofission and Photoneutron Cross Sections and Photofission Neutron Multiplicities for U^{233}, U^{234}, Np^{237} and Pu^{239},* Phys Rev C34, 6, 2201-2214 (Dec 1986).
10. P. Brown, *Solving the Nuclear Waste Problem Through Applied Physics*, Advanced Energy Symposium, August 14-15, 1998, Salt Lake City, UT.
11. P. Brown, *Neutralizing Nuclear Waste Using Applied Physics*, Infinite Energy 4, 21, 9-13 (1998).
12. P. Brown, *Transmutation of Nuclear Waste Products Using Giant Dipole Resonant Gamma Rays*, Cold Fusion & New Energy Symposium, Manchester, NH, Oct 11, 1998.
13. P. Brown, *Solving the Nuclear Waste Problem Through Applied Physics*, J. of New Energy 3, 2/3, 38-46 (1998).
14. P. Brown, *Transmutation of Nuclear Waste Products Using Giant Dipole Resonant Gamma Rays*, Infinite Energy 4, 23, 44-46 (1999).
15. T. Kase, et.al., *Product Yileds of U^{235}, U^{238}, NP^{237}, and Pu^{239} by Photofission Reactions with 20, 30 and 60 MeV Bremsstrahlung*, Nuclear Science & Engineering 111, 368-378 (1992).
16. Y. Wang, et.al., *Study of Characteristics of Linac with TWRR*, The 9th Symp. Accel. Sci. & Tech., Tsukuba, Japan 1993.
17. S. Toyama, *High Power CW Linac in PNC*, Proceedings of the 15th Biennial Particle Accelerator Conference, Wash, DC, 1993.
18. M. Nomura, et.al., *Status of High Power CW Linac at PNC*, Proceedings of the 18th Linear Accelerator Meeting.
19. T. Kase, et.al., *An Assessment of the Continuous Neutron Source Using a Low-Energy Electron Accelerator*, Nuclear Science & Engineering 126, 59-70 (1997).
20. Y. Wang, *Design of High power Electron Linac at PNC*, J. Nucl. Sci., & Tech. 30 (12), 1261-1274 (Dec 1993).
21. T. Matsumoto, *Calculation of Gamma Ray Incineration of Sr^{90} and Cs^{137}*, Nucl. Instru. & Methods in Phys. Res. A268, 234-243 (1988).

22. P. Brown, *Effective Radioactive Waste Remediation*, International Conference on Future Energy, April 29-May 1, 1999, Bethesda, MD.